

# COLLECTIVE EFFECTS IN PULSED BEAM FREE-ELECTRON LASERS OPERATING IN THE TERA-HERTZ REGIME\*

Y. Pinhasi<sup>#</sup>, Yu. Lurie, Ariel University Center of Samaria, Ariel 40700, Israel

## Abstract

Intense radiation devices such as microwave tubes, free-electron lasers (FELs) and masers, utilize distributed interaction between an electron beam and the electromagnetic field. Our space-frequency theory is extended to consider collective effects emerging while ultra short electron pulses are propagating in the interaction region. The total electromagnetic field (radiation and space-charge waves) is presented in the frequency domain as an expansion in terms of transverse eigen-modes. The mutual interaction between the electron beam and the electromagnetic field is fully described by a set of coupled equations, expressing the evolution of mode amplitudes and electron beam dynamics.

The model is used for the analysis and simulation of radiation excitation and propagation in pulsed beam free-electron lasers operating in millimeter wavelengths and in the Tera-Hertz frequencies. The approach is applied in a numerical particle code WB3D, simulating wide-band interaction of a free-electron laser operating in the linear and non-linear regimes. The model is utilized to study spontaneous and super-radiant emissions radiated by an electron bunch at the sub-millimeter regime, taking into account three dimensional space-charge effects playing a role in such ultra short bunches.

## INTRODUCTION

Electron devices such as microwave tubes and free-electron lasers (FELs) utilize distributed interaction between an electron beam and electromagnetic radiation. Many models have been developed to describe the mutual interaction between the gain medium (electron beam) and the excited radiation. These models are based on a solution of Maxwell equations and the Lorenz force equation in the time domain. Contrary to space-time models, formulation of the electromagnetic excitation equations in the frequency domain inherently takes into account dispersive effects arising from the cavity and the gain medium. Moreover, it facilitates consideration of the statistical features of the electron beam and the excited radiation, necessary for the study of spontaneous emission, synchrotron amplified spontaneous emission (SASE), super-radiance and noise.

In this paper we develop a space-frequency model, which describes broadband phenomena occurring in electron devices, masers and FELs and characterized by a continuum of frequencies. The total electromagnetic field is presented in the frequency domain as a summation of transverse eigen-modes of the cavity, in which it is excited and propagates. A set of coupled excitation equations, describing the evolution of each transverse mode, is solved self-consistently with beam dynamics equations. This coupled-mode model is employed in a

three-dimensional numerical simulation WB3D [1,2]. The code was used to study the statistical and spectral characteristics of the radiation generated in a pulsed beam free-electron laser, operating in the millimeter and sub-millimeter wavelengths.

## PRESENTATION OF THE ELECTROMAGNETIC FIELD IN THE FREQUENCY DOMAIN

The electromagnetic field in the time domain is described by the space-time electric  $\mathbf{E}(\mathbf{r}, t)$  and magnetic  $\mathbf{H}(\mathbf{r}, t)$  signal vectors.  $\mathbf{r}$  stands for the  $(x, y, z)$  coordinates, where  $(x, y)$  are the transverse coordinates and  $z$  is the axis of propagation. The Fourier transform of the electric field is defined by:

$$\mathbf{E}(\mathbf{r}, f) = \int_{-\infty}^{+\infty} \mathbf{E}(\mathbf{r}, t) e^{+j2\pi f t} dt \quad (1)$$

where  $f$  denotes the frequency. Similar expression is defined for the Fourier transform  $\mathbf{H}(\mathbf{r}, f)$  of the magnetic field. Since the electromagnetic signal is real (i.e.  $\mathbf{E}^*(\mathbf{r}, t) = \mathbf{E}(\mathbf{r}, t)$ ), its Fourier transform satisfies  $\mathbf{E}^*(\mathbf{r}, f) = \mathbf{E}(\mathbf{r}, -f)$ .

Analytic representation of the signal is given by the complex expression [2]:

$$\tilde{\mathbf{E}}(\mathbf{r}, t) \equiv \mathbf{E}(\mathbf{r}, t) - j\hat{\mathbf{E}}(\mathbf{r}, t) \quad (2)$$

where

$$\hat{\mathbf{E}}(\mathbf{r}, t) = \frac{1}{\pi} \int_{-\infty}^{+\infty} \frac{\mathbf{E}(\mathbf{r}, t')}{t-t'} dt' \quad (3)$$

is the Hilbert transform of  $\mathbf{E}(\mathbf{r}, t)$ . Fourier transformation of the analytic representation (2) results in a "phasor-like" function  $\tilde{\mathbf{E}}(\mathbf{r}, f)$  defined in the positive frequency domain and related to the Fourier transform by:

$$\tilde{\mathbf{E}}(\mathbf{r}, f) = 2\mathbf{E}(\mathbf{r}, f) \cdot u(f) = \begin{cases} 2\mathbf{E}(\mathbf{r}, f) & f > 0 \\ 0 & f < 0 \end{cases} \quad (4)$$

The Fourier transform can be decomposed in terms of the "phasor like" functions according to:

$$\mathbf{E}(\mathbf{r}, f) = \frac{1}{2}\tilde{\mathbf{E}}(\mathbf{r}, f) + \frac{1}{2}\tilde{\mathbf{E}}^*(\mathbf{r}, -f) \quad (5)$$

and the inverse Fourier transform is then:

$$\begin{aligned} \mathbf{E}(\mathbf{r}, t) &= \int_{-\infty}^{+\infty} \mathbf{E}(\mathbf{r}, f) e^{-j2\pi f t} df \\ &= \text{Re} \left\{ \int_0^{+\infty} \tilde{\mathbf{E}}(\mathbf{r}, f) e^{-j2\pi f t} df \right\} \end{aligned} \quad (6)$$

### THE WIENER-KHINCHINE AND PARSEVAL THEOREMS FOR ELECTROMAGNETIC FIELDS

The cross-correlation function of the time dependent electric  $\mathbf{E}(\mathbf{r}, t)$  and magnetic  $\mathbf{H}(\mathbf{r}, t)$  fields is given by:

$$R_{EH}(z, \tau) = \int_{-\infty}^{+\infty} \{ \iint [\mathbf{E}(\mathbf{r}, t + \tau) \times \mathbf{H}(\mathbf{r}, t)] \cdot \hat{\mathbf{z}} dx dy \} dt \quad (7)$$

Note that for finite energy signals, the total energy carried by the electromagnetic field is given by  $W(z) = R_{EH}(z, 0)$ .

According to the Wiener-Khinchine theorem, the spectral density function of the electromagnetic signal energy  $S_{EH}(z, f)$  is related to the Fourier transform of the cross-correlation function  $R_{EH}(z, \tau)$  through the Fourier transformation:

$$\begin{aligned} S_{EH}(z, f) &= \int_{-\infty}^{+\infty} R_{EH}(z, \tau) e^{+j2\pi f \tau} d\tau \\ &= \iint [\mathbf{E}(\mathbf{r}, f) \times \mathbf{H}^*(\mathbf{r}, f)] \cdot \hat{\mathbf{z}} dx dy \\ &= \begin{cases} \frac{1}{4} \iint [\tilde{\mathbf{E}}(\mathbf{r}, f) \times \tilde{\mathbf{H}}^*(\mathbf{r}, f)] \cdot \hat{\mathbf{z}} dx dy & f > 0 \\ \frac{1}{4} \iint [\tilde{\mathbf{E}}(\mathbf{r}, -f) \times \tilde{\mathbf{H}}^*(\mathbf{r}, -f)] \cdot \hat{\mathbf{z}} dx dy & f < 0 \end{cases} \end{aligned} \quad (8)$$

Following Parseval theorem, the total energy carried by the electromagnetic field can also be calculated by integrating the spectral density  $S_{EH}(z, f)$  over the entire frequency domain:

$$\begin{aligned} W(z) &= \int_{-\infty}^{+\infty} S_{EH}(z, f) df \\ &= \int_0^{+\infty} \left[ \frac{1}{2} \iint \text{Re} \{ \tilde{\mathbf{E}}(\mathbf{r}, f) \times \tilde{\mathbf{H}}^*(\mathbf{r}, f) \} \cdot \hat{\mathbf{z}} dx dy \right] df \end{aligned} \quad (9)$$

We identify:

$$\frac{dW(z)}{df} = \frac{1}{2} \text{Re} \left\{ \iint [\tilde{\mathbf{E}}(\mathbf{r}, f) \times \tilde{\mathbf{H}}^*(\mathbf{r}, f)] \cdot \hat{\mathbf{z}} dx dy \right\} \quad (10)$$

as the spectral energy distribution of the electromagnetic field (over positive frequencies).

### MODAL PRESENTATION OF ELECTROMAGNETIC FIELD IN THE FREQUENCY DOMAIN

The ‘‘phasor like’’ quantities defined in (4) can be expanded in terms of transverse eigenmodes of the medium in which the field is excited and propagates [3]-

**FEL Theory**

100

[5]. The perpendicular component of the electric and magnetic fields are given in any cross-section as a linear superposition of a complete set of transverse eigenmodes:

$$\tilde{\mathbf{E}}_{\perp}(\mathbf{r}, f) = \sum_q \begin{bmatrix} C_{+q}(z, f) e^{+jk_{zq} z} \\ + C_{-q}(z, f) e^{-jk_{zq} z} \end{bmatrix} \tilde{\mathcal{E}}_{q\perp}(x, y) \quad (11)$$

$$\tilde{\mathbf{H}}_{\perp}(\mathbf{r}, f) = \sum_q \begin{bmatrix} C_{+q}(z, f) e^{+jk_{zq} z} \\ - C_{-q}(z, f) e^{-jk_{zq} z} \end{bmatrix} \tilde{\mathcal{H}}_{q\perp}(x, y)$$

$C_{+q}(z, f)$  and  $C_{-q}(z, f)$  are scalar amplitudes of the  $q$ th forward and backward modes respectively with electric field  $\tilde{\mathcal{E}}_{q\perp}(x, y)$  and magnetic field  $\tilde{\mathcal{H}}_{q\perp}(x, y)$  profiles and axial wavenumber:

$$k_{zq} = \begin{cases} \sqrt{k^2 - k_{\perp q}^2} & k > k_{\perp q} \text{ (prop. modes)} \\ j\sqrt{k_{\perp q}^2 - k^2} & k < k_{\perp q} \text{ (cut-off modes)} \end{cases} \quad (12)$$

Expressions for the longitudinal component of the electric and magnetic fields are obtained after substituting the modal representation (11) of the fields into Maxwell's equations, where source of electric current density  $\tilde{\mathbf{J}}(\mathbf{r}, f)$  is introduced:

$$\begin{aligned} \tilde{\mathbf{E}}_z(\mathbf{r}, f) &= \sum_q \begin{bmatrix} C_{+q}(z, f) e^{+jk_{zq} z} \\ - C_{-q}(z, f) e^{-jk_{zq} z} \end{bmatrix} \tilde{\mathcal{E}}_{qz}(x, y) \\ &\quad + \frac{1}{j2\pi f \epsilon_0} \underbrace{\tilde{\mathcal{J}}_z(\mathbf{r}, f)}_{\Delta \tilde{\mathcal{E}}_z(\mathbf{r}, f)} \end{aligned} \quad (13)$$

$$\tilde{\mathbf{H}}_z(\mathbf{r}, f) = \sum_q \begin{bmatrix} C_{+q}(z, f) e^{+jk_{zq} z} \\ + C_{-q}(z, f) e^{-jk_{zq} z} \end{bmatrix} \tilde{\mathcal{H}}_{qz}(x, y)$$

The evolution of the amplitudes of the excited modes is described by a set of coupled differential equations:

$$\frac{d}{dz} C_{\pm q}(z, f) = \mp \frac{1}{\mathcal{N}_q} e^{\mp jk_{zq} z} \times \quad (14)$$

$$\times \iint \left[ \frac{Z_q}{Z_q^*} \tilde{\mathbf{J}}_{\perp}(\mathbf{r}, f) \pm \hat{\mathbf{z}} \tilde{\mathcal{J}}_z(\mathbf{r}, f) \right] \cdot \tilde{\mathcal{E}}_q^*(x, y) dx dy$$

The normalization of the field amplitudes of each mode is made via each mode's complex Poynting vector power:

$$\mathcal{N}_q = \iint [\tilde{\mathcal{E}}_{q\perp}(x, y) \times \tilde{\mathcal{H}}_{q\perp}^*(x, y)] \cdot \hat{\mathbf{z}} dx dy \quad (15)$$

and the mode impedance is given by:

$$Z_q = \begin{cases} \sqrt{\frac{\mu_0}{\epsilon_0}} \frac{k}{k_{zq}} = \frac{2\pi f \mu_0}{k_{zq}} & \text{for TE modes} \\ \sqrt{\frac{\mu_0}{\epsilon_0}} \frac{k_{zq}}{k} = \frac{k_{zq}}{2\pi f \epsilon_0} & \text{for TM modes} \end{cases} \quad (16)$$

Substituting the expansion (11) in (10) results in an expression for the spectral energy distribution of the electromagnetic field (over positive frequencies) as a sum of energy spectrum of the excited modes:

$$\frac{dW(z)}{df} = \sum_{q, \text{ Prop.}} \frac{1}{2} \left[ |C_{+q}(z, f)|^2 - |C_{-q}(z, f)|^2 \right] \cdot \text{Re}\{\mathcal{N}_q\} + \sum_{q, \text{ Cut-off}} \text{Im}\{C_{+q}(z, f)C_{-q}^*(z, f)\} \cdot \text{Im}\{\mathcal{N}_q\} \quad (17)$$

The expressions for the perpendicular and longitudinal components of the electric field also include the full three-dimensional description of space-charge forces due to collective effects in the electron beam. In electron devices and free-electron lasers, the electron beam is usually magnetically confined in the transverse direction. This allows a common approximation in which transverse variation of the current density is neglected, i.e.  $|\nabla_{\perp} \cdot \tilde{\mathbf{J}}_{\perp}| \ll |\partial \tilde{J}_z / \partial z|$ . In this case, the longitudinal electric field (13) gives rise to the dominant part of space-charge forces along the e-beam pulse. Modal description of  $\tilde{E}_z(\mathbf{r}, f)$  consists of a summation over TM modes of the waveguide and the additional term  $\Delta \tilde{E}_z(\mathbf{r}, f) = \tilde{J}_z(\mathbf{r}, f) / [j2\pi f \epsilon_0]$  identified as the longitudinal space-charge field in a 1D description. A comprehensive discussion on the modeling of space-charge in free-electron lasers is given in reference [6] appearing in this issue.

## NUMERICAL RESULTS

When the electron beam is pre-bunched to short pulses, the fields excited by the electrons become correlated and coherent summation of radiation fields from individual particles occurs. All electrons radiate in phase with each other in this situation, and the generated radiation is termed as super-radiant emission [7-9]. It was shown that energy flux of super-radiant emission is proportional to the square of the total charge  $Q_b$  of the driving electron pulse and to the square of the interaction length  $L_w$ . However if the charge density is increased, collective effects force the bunch to expand along the interaction region, causing the particles to lose their initial phase coherence. As the temporal duration of the electron pulse approaches the period of the emitted radiation, the super-radiance effect is suppressed and the spontaneous emission becomes dominant. The energy flux of

spontaneous emission is proportional to the bunch charge  $Q_b$ .

We use WB3D numerical code [1,2] to simulate pulsed beam FEL radiation in the sub-millimeter wavelengths. The parameters of the FEL are summarized in Table 1. Trajectories of electrons obtained in the simulations with bunch charges of  $Q_b=30\text{pC}$  and  $0.5\text{nC}$  are demonstrated in the figure 1. At the entrance to interaction region, the pulse  $T_b$  is relatively short so as  $f_s T_b \ll 1$  ( $f_s$  is the frequency of the emitted radiation at synchronism), resulting in a strong super-radiant emission. As the electron bunch propagates along the wiggler, its temporal duration increases due to the space-charge forces, as clearly seen in the Fig. 1. When the temporal bunch width becomes  $f_s T_b \geq 1$ , only spontaneous emission takes place in the following stages of the interaction.

The situation is illustrated in figure 2, describing the evolution of the energy flux spectral density of the radiation emitted along the interaction region. When the bunch charge is  $Q_b=30\text{pC}$ , the expansion of the bunch due to space-charge forces is relatively small, and the cumulative contribution of a longer interaction path to the radiation is considerable. However, as the charge of the bunch is increased (to  $Q_b=1\text{nC}$ ), space-charge forces give rise to a fast expansion of the electron pulse so the most part of the radiation is emitted only at the first stages of the wiggler.

In order to measure the phase coherence between the particles, we define a bunching factor:

$$b(z) \equiv \left\langle e^{j2\pi f_s t_i(z)} \right\rangle = \frac{1}{N} \sum_{i=1}^N e^{j2\pi f_s t_i(z)} \quad (18)$$

and draw it along the interaction region, as shown in figure 3. If low-charge electron bunches are applied, the bunching factor remains relatively high along the most part of its path of propagation, generating an intensified super-radiant emission. The total energy flux  $W_{tot}$  grows fast along the wiggler. Increasing of the bunch charge leads to a fast reduction of the bunching factor even at the very first stage of the radiation buildup process, what results in a destruction of the emission coherence and a low energy flux.

Table 1: Parameters of pulsed beam FEL operating in the sub-millimeter band.

### Accelerator

Electron beam energy:	$E_k = 5.5\text{ MeV}$
Initial pulse duration:	$T_b = 0.05\text{ pS}$
Pulse charge:	$Q_b = 30\text{ pC} \div 1\text{ nC}$

### Wiggler

Magnetic induction:	$B_w = 2000\text{ G}$
Period:	$\lambda_w = 2.5\text{ cm}$
Number of periods:	$N_w = 20$

### Waveguide

Rectangular waveguide:	$15 \times 10\text{ mm}^2$
------------------------	----------------------------

REFERENCES

- [1] Y. Pinhasi, Yu. Lurie and A. Yahalom, Nucl. Instr. and Meth. in Phys. Res. A **475** (2001), p.147.
- [2] Y. Pinhasi, Yu. Lurie, A. Yahalom, Phys. Rev. E **71**, (2005), 036503.
- [3] N. Markovitz and J. Schwinger, J. Appl. Phys. **22** (1951), 806.
- [4] L. B. Felsen, *Radiation and scattering of waves* (Prentice Hall, New Jerzy, 1973).
- [5] L. A. Vaynshteyn, *Electromagnetic waves* (Sovietskoye Radio, Moscow, 1957).
- [6] Yu. Lurie, Y. Pinhasi, MOP26 in this issue.
- [7] R.H. Dicke, Phys. Rev. **93** (1954), 99;
- [8] A. Gover *et al.*, Phys. Rev. Lett. **72** (1994), 1192;
- [9] Y. Pinhasi, and Yu. Lurie, Phys. Rev. E **65**, Issue 2 (2002) p. 026501.

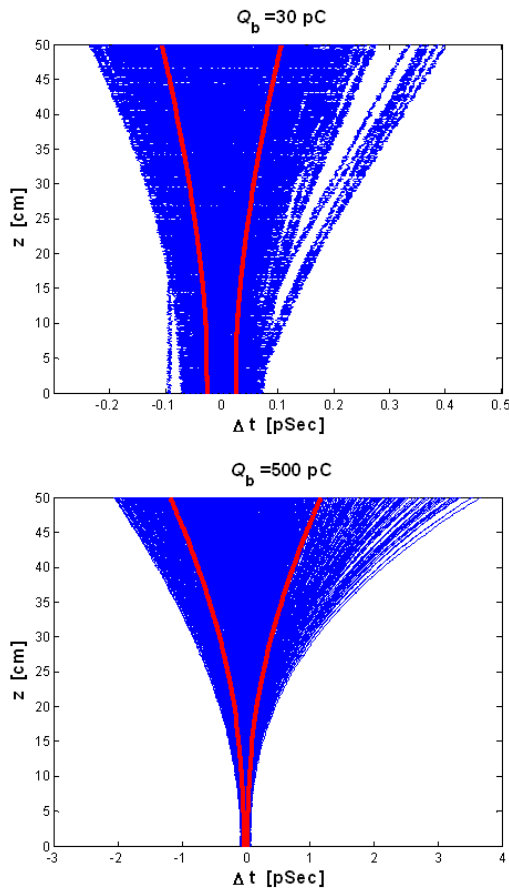


Figure 1: Electron trajectories along the interaction region relative to the bunch center in simulations with bunch charges  $Q_b=30 \text{ pC}$  (left) and  $0.5 \text{ nC}$  (right). Red lines show RMS pulse widths.

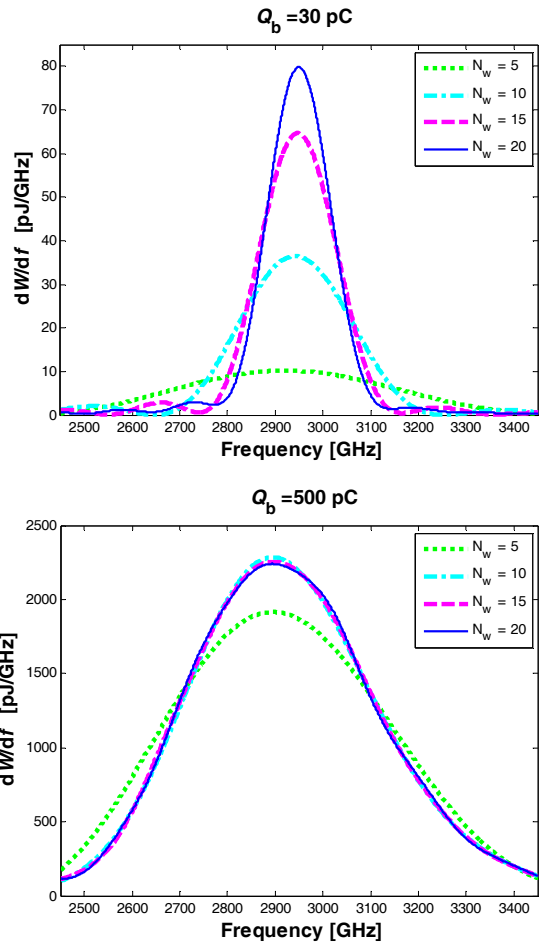


Figure 2: Evolution of energy flux spectral density for  $Q_b=30 \text{ pC}$  (left) and  $0.5 \text{ nC}$  (right).

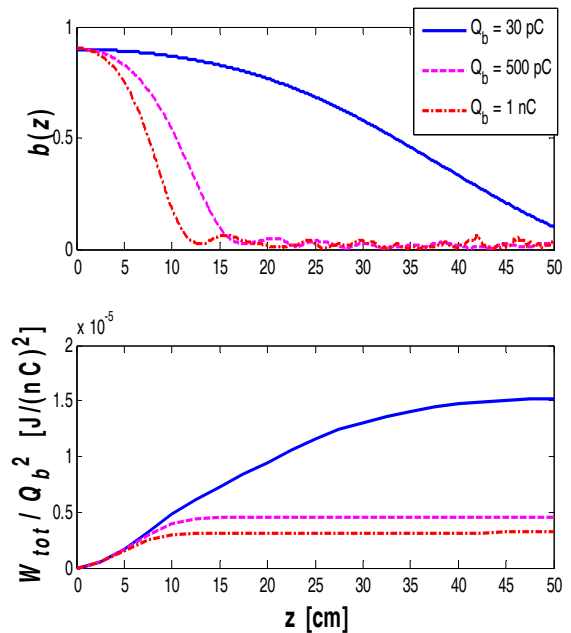


Figure 3: Bunching factor  $b(z)$  and normalized total energy flux for different pulse charges.